

Supplementary Information

Ytterbium Can Relax Slowly Too : Field induced Yb₂ Single-Molecule Magnet.

Po-Heng Lin,^a Wen-Bin Sun,^{b*} Yong-Mei Tian,^b Peng-Fei Yan,^{b*} Liviu Ungur,^c Liviu. F. Chibotaru^{c*} and Muralee Murugesu^{a*}

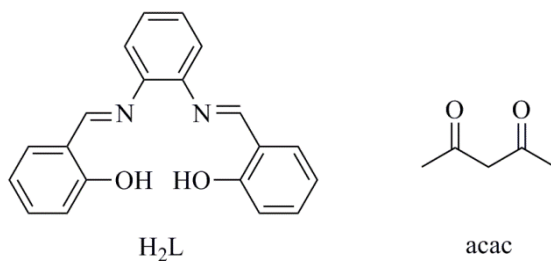
University of Ottawa, Department of Chemistry, 10 Marie Curie, Ottawa, ON, K1N6N5,
Canada.

Key Laboratory of Functional Inorganic Material Chemistry, Ministry of Education, No.
74, Xuefu Road, Nangang District, Harbin 150080, PR China.

Division of Quantum and Physical Chemistry and INPAC—Institute for Nanoscale
Physics and Chemistry, Katholieke Universiteit Leuven, Celestijnenlaan, 200F, 3001,
Belgium.

Preparation of N,N-bis(salicylidene)-*o*-phenylenediamine:

The salen-type ligand, N,N'-bis(salicylidene)-*o*-phenylenediamine (H₂L), was obtained by using previously reported synthetic methods.¹



Scheme S1. Representation of the salen-type (H₂L) and acac ligands

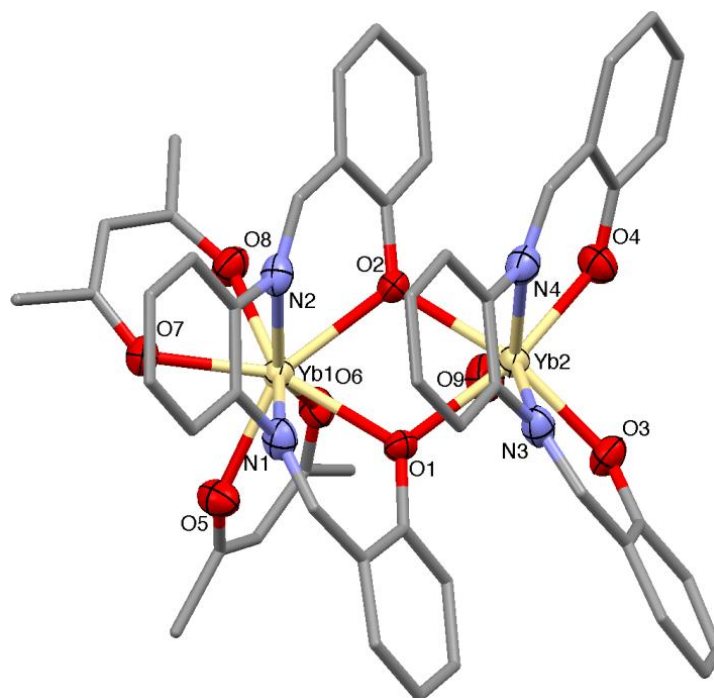


Figure S1. Partially labelled molecular structure of [Yb₂L₂(acac)₂(H₂O)], **1**. Yb1 is in a distorted square antiprism environment, Yb2 is in a distorted capped trigonal prism environment. Colour code: Yb (yellow), O (red), N (blue) C (grey). H atoms were omitted for clarity.

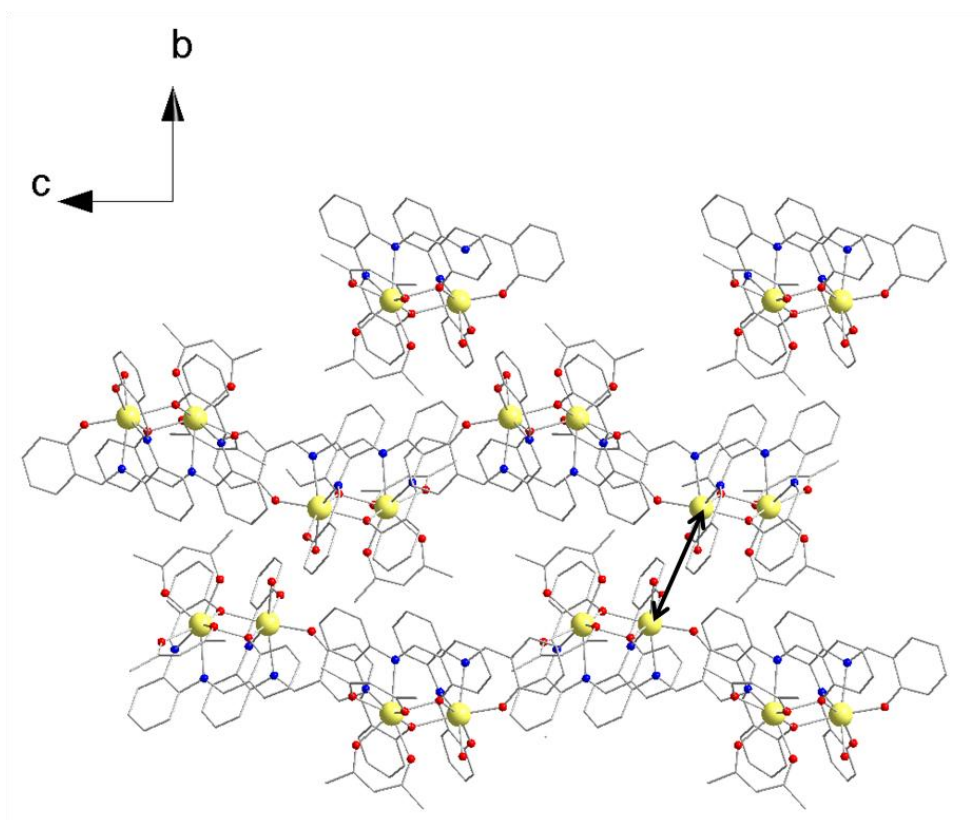


Figure S2. Crystal packing diagram of complex **1** along the crystallographic *a* axis. The arrow shows the closest intramolecular contact between Yb2...Yb2a (5.94 Å). Colour code: Yb (yellow), O (red), N (blue) C (grey). H atoms were omitted for clarity.

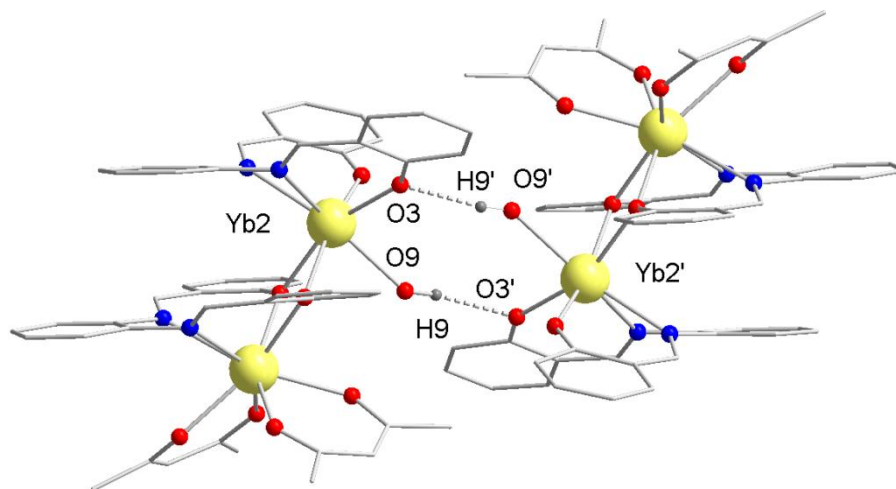


Figure S3. The two hydrogens bonds between two neighboring molecules. Colour code: The two hydrogens bonds between two neighboring molecules. Colour code: Yb (Yellow), O (red), N (blue) C (grey) and Black (H).

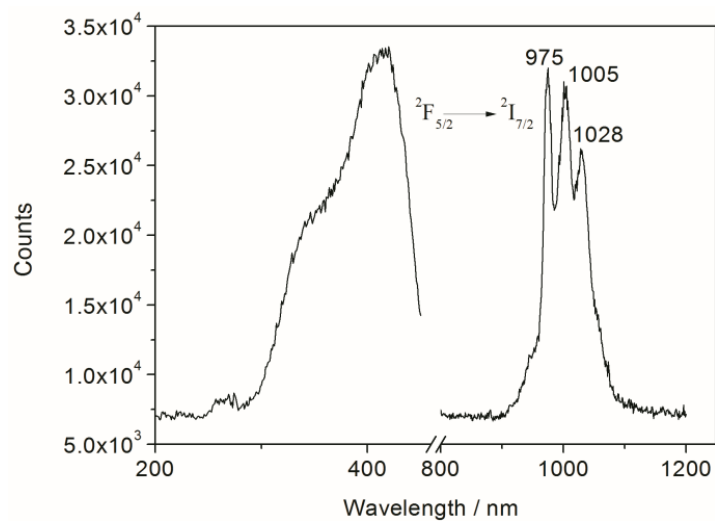


Figure S4. The NIR fluorescence of **1** in CH_2Cl_2 (1.0×10^{-5} M).

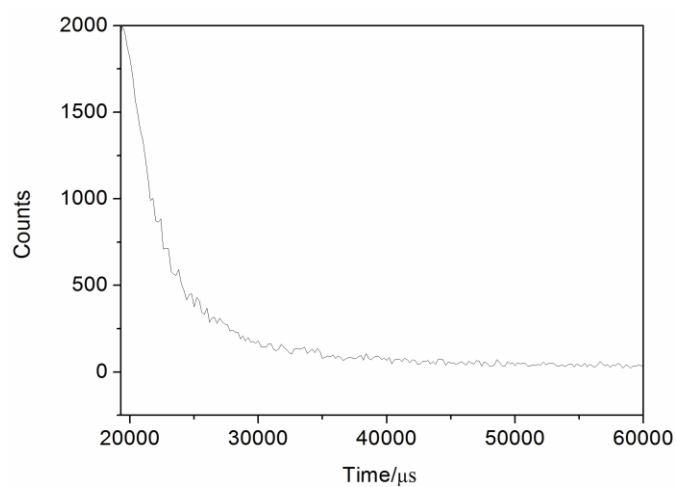


Figure S5. The decay curve of excited states for lifetime value of **1** in CH_2Cl_2 at room temperature.

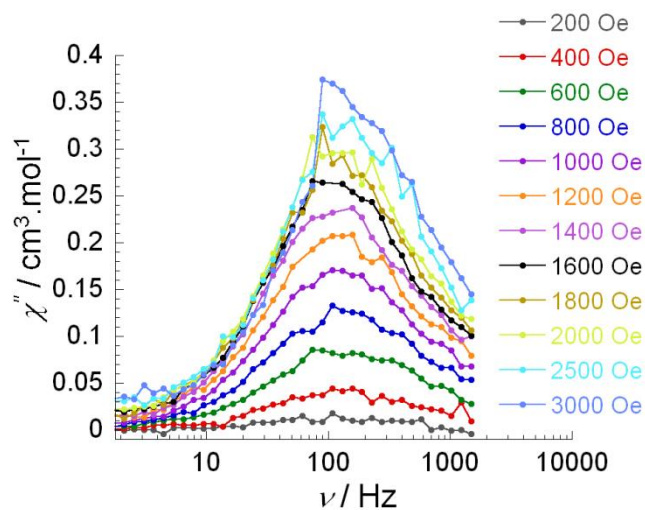


Figure S6. Out-of-phase susceptibility χ'' vs. frequency ν in the field range 0 - 3000 Oe for complex 1.

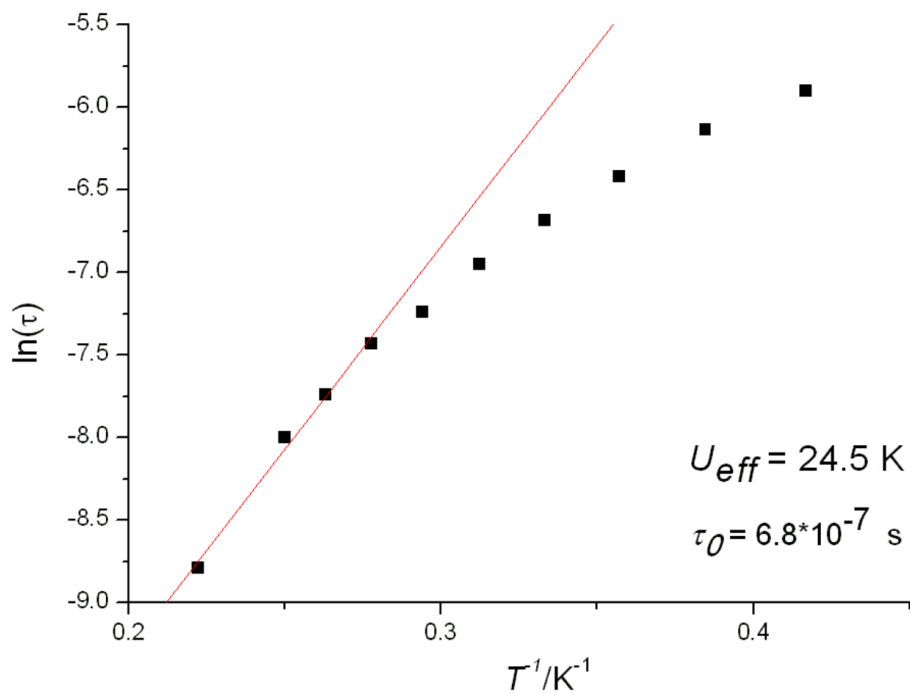


Figure S7. $\ln(\tau)$ vs. T^{-1} plot at H_{dc} 1600 Oe representing thermally activated relaxation regime. The solid lines represent an Arrhenius fit of the data.

Computational details

All calculations were done with MOLCAS 7.6 and are of CASSCF/RASSI/SINGLE_ANISO type.

Computational models:

We have employed 2 structural approximations for each fragment Yb1 and Yb2: (**A** – a reduced fragment of the molecule and **B** – the entire molecule) and 2 basis set approximations (**1** –small and **2**-large), resulting in 4 computational approximations for molecule Yb₂ (**A1**, **A2**, **B1**, **B2**).

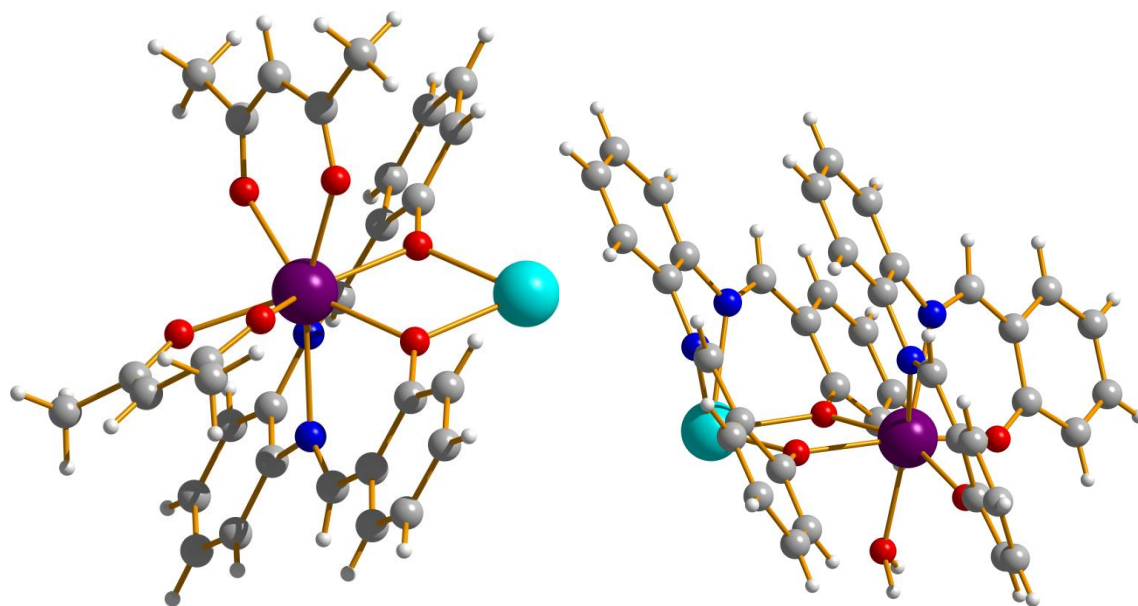


Figure S8. Structure of the fragments **A** (right - Yb1, left - Yb2) of the complex Yb₂. Color scheme: Yb - violet, La – light turquoise, N – blue, O – red, C – grey, H – white.

Table S1. Contractions of the employed basis sets in computational approximations **1** and **2**.

Basis 1	Basis 2
Yb.ANO-RCC...7s6p4d3f1g.	Yb.ANO-RCC...8s7p5d4f2g1h.
La.ECP.deGraaf.0s.0s.0e-La(LaMnO3).	La.ECP.deGraaf.0s.0s.0e-La(LaMnO3).
Lu.ANO-RCC...7s6p4d3f1g.	Lu.ANO-RCC...7s6p4d3f1g.
O.ANO-RCC...3s2p1d. (close)	O.ANO-RCC...4s3p2d. (close)
O.ANO-DK3.Tsuchiya.12s8p.2s1p. (distant)	O.ANO-RCC...3s2p. (distant)
N.ANO-RCC...3s2p1d. (close)	N.ANO-RCC...4s3p2d. (close)
N.ANO-DK3.Tsuchiya.12s8p.2s1p. (distant)	N.ANO-RCC...3s2p. (distant)
C.ANO-DK3.Tsuchiya.12s8p.2s1p.	C.ANO-RCC...3s2p.
H.ANO-DK3.Tsuchiya.6s.1s.	H.ANO-RCC...2s.

Active space of the CASSCF method included 13 electrons in 7 orbitals (4f orbitals of Yb³⁺ ion).

We have mixed 7 (all) doublet states by spin-orbit coupling.

On the basis of the resulting spin-orbital multiplets SINGLE_ANISO program computed local magnetic properties (g-tensors, magnetic axes, local magnetic susceptibility, etc.) The program POLY_ANISO computed the exchange spectrum and the magnetic properties of the dimer.

Table S2. Energies (cm^{-1}) and g tensors of the lowest Kramers doublets (KD).

Center Yb1:

KD		A1		A2		B1		B2	
		E	g	E	g	E	g	E	g
1	gx		0.7535		0.7981		0.9589		0.9928
	gy	0.000	1.8032	0.000	1.7566	0.000	1.8002	0.000	1.8549
	gz		5.5557		5.5748		6.1164		5.9508
2	gx		0.4490		1.3024		1.3521		1.6832
	gy	167.350	1.4623	176.508	2.5822	190.491	2.3911	189.051	2.0574
	gz		5.4069		4.1061		3.8016		4.0340
3	gx		0.4103		0.5872		0.3459		0.0547
	gy	193.747	1.1712	210.833	1.4094	281.227	0.7774	287.500	0.8393
	gz		5.3322		6.4771		5.9109		6.4418
4	gx		0.1508		0.1088		0.3383		0.2371
	gy	353.267	0.3557	368.142	0.2797	366.083	0.5861	368.463	0.5015
	gz		7.5950		7.6600		7.0809		7.2326

Center Yb2:

KD		A1		A2		B1		B2	
		E	g	E	g	E	g	E	g
1	gx		0.1586		0.2079		0.3516		0.3852
	gy	0.000	1.2241	0.000	0.9301	0.000	1.0588	0.000	0.9707
	gz		6.7491		7.1406		7.0683		7.1998
2	gx		3.7271		4.0783		4.6849		4.4380
	gy	239.769	3.2701	310.566	2.9533	292.947	3.2959	336.958	3.3772
	gz		0.1948		0.2906		1.0972		1.3410
3	gx		0.4871		0.9129		0.0897		0.2195
	gy	353.371	1.7251	430.746	1.9830	485.888	1.0006	539.921	1.2105
	gz		5.1016		5.9542		6.0237		6.1096
4	gx		0.0646		0.0277		0.4713		0.4504
	gy	595.182	0.1815	664.731	0.0988	591.200	0.9833	645.598	1.1120
	gz		7.7980		7.8212		7.2086		7.1132

Table S3. Angles between the g_z axes of the lowest Kramers doublets (KD) in all computational models (degrees).

center	mode	center Yb1				center Yb2			
		A1	A2	B1	B2	A1	A2	B1	B2
Yb1	A1	0.000	0.391	28.040	25.887	135.67 5	136.76 3	135.00 3	135.67 8
	A2	0.391	0.000	28.379	26.228	135.32 5	136.41 8	134.65 1	135.32 8
	B1	28.040	28.379	0.000	2.167	163.60 2	164.77 3	162.86 2	163.59 0
	B2	25.887	26.228	2.167	0.000	161.49 7	162.63 8	160.77 5	161.48 9
Yb2	A1	135.67 5	135.32 5	163.60 2	161.49 7	0.000	1.584	0.948	0.150
	A2	136.76 3	136.41 8	164.77 3	162.63 8	1.584	0.000	2.531	1.693
	B1	135.00 3	134.65 1	162.86 2	160.77 5	0.948	2.531	0.000	0.851
	B2	135.67 8	135.32 8	163.59 0	161.48 9	0.150	1.693	0.851	0.000

Table S4. Energies and the corresponding tunneling gaps of the lowest 4 exchange doublet states of the complex Yb_2 .

A1		A2		B1		B2	
energy	Δ_t	energy	Δ_t	energy	Δ_t	energy	Δ_t
0.00000000 0.01485504	1.4855E-02	0.00000000 0.01159313	1.1593E-02	0.00000000 0.01282147	1.2821E-02	0.00000000 0.01189421	1.1894E-02
0.12655795 0.14729532	2.0737E-02	0.13602336 0.15357224	1.7549E-02	0.15408078 0.17536270	2.1282E-02	0.15445619 0.17542771	2.0972E-02
167.34771880 167.37159324	2.3874E-02	176.52952647 176.57500080	4.5474E-02	190.52159106 190.56716357	4.5573E-02	189.08635133 189.13064831	4.4297E-02
167.47314081 167.49850140	2.5361E-02	176.58982768 176.64039430	5.0567E-02	190.58279051 190.63472791	5.1937E-02	189.13857178 189.19102023	5.2448E-02

i (a) C. Subrahmanyam, M. Seshasayee and G. Aravamudan, *G. Cryst. Struct. Commun.* 1982, **11**, 1719. (b) K. Ambroziak, Z. Rozwadowski, T. Dziembowska, and B. J. Bieg, *Mol. Struct.* 2002, **615**, 109.